ACS SENSORS

pubs.acs.org/acssensors Article

Connecting Artificial Proteolytic and Electrochemical Signaling Systems with Caged Messenger Peptides

Paolo Bollella, Selvakumar Edwardraja, Zhong Guo, Claudia E. Vickers, Jason Whitfield, Patricia Walden, Artem Melman, Kirill Alexandrov,* and Evgeny Katz*

Cite This: *ACS Sens.* 2021, 6, 3596–3603 Read Online

ACCESS | Metrics & More | Article Recommendations | Supporting Information

ABSTRACT: Enzymatic polypeptide proteolysis is a widespread and powerful biological control mechanism. Over the last few years, substantial progress has been made in creating artificial proteolytic systems where an input of choice modulates the protease activity and thereby the activity of its substrates. However, all proteolytic systems developed so far have relied on the direct proteolytic cleavage of their effectors. Here, we propose a new concept where protease biosensors with a tunable input uncage a signaling peptide, which can then transmit a signal to an allosteric protein reporter. We demonstrate that both the cage and the regulatory domain of the reporter can be constructed from the same peptide-binding domain, such as calmodulin. To demonstrate this concept, we constructed a proteolytic rapamycin biosensor and demonstrated its quantitative actuation on fluorescent, luminescent, and electrochemical reporters. Using the latter, we constructed sensitive bioelectrodes that detect the messenger peptide release and quantitatively convert the recognition event into electric current. We discuss the application of such systems for the construction of *in vitro* sensory arrays and *in vivo* signaling circuits.

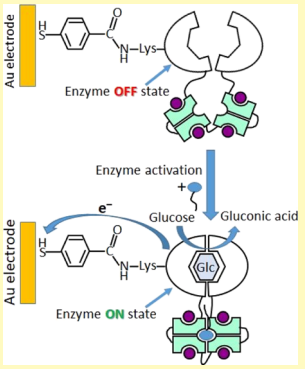

KEYWORDS: *biosensor, proteinase, chimeric enzyme, allostery, switchable enzyme, rapamycin*

INTRODUCTION

Living organisms maintain their homeostasis through a network of interwoven signaling and metabolic systems. While fundamentally all of them are built on the gene expression controlling the type and amount of the components delivered into the system, many biological processes occur on time scales much faster (milliseconds to seconds) than those of gene expression (minutes to hours). As a result, biological systems possess a range of rapid and, predominately, protein-based signaling systems that can respond to metabolic and environmental changes in real time. There has been a sustained effort to create artificial metabolic and signaling networks as part of both academic engineering efforts and the biotechnological innovation in diagnostics, biochemical engineering, and bioelectronics.[1] Initially, new pathways were constructed from naturally occurring enzymes combined in unnatural ways in order to achieve the desired chemical transformations or signal propagation.[2,3] This approach is complicated by the mismatch in chemistries as well as properties of the natural enzymes such as the stability, optimal pH, and ionic strength, cofactor requirements, and the kinetic parameters. The advent of synthetic biology has sparked numerous efforts to construct biochemical cascades based on engineered protein switches. This approach holds potential for creating orthogonal signaling systems that connect biochemical networks to nonbiological information processing systems such as electronics, including implantable[4] and wearable[5] bioelectronics. The protein switch engineering efforts have focused on several types of reporter domains: light-emitting proteins such as fluorescent proteins and luciferases, redox enzymes that can be monitored electrochemically, and finally enzymes that can actuate on colorimetric reactions.[6−10] Among the enzymes capable of generating easily measurable outputs, proteases have a special place due to the dramatic changes in the physical properties of their substrates, high and engineerable substrate specificity, natural orthogonality, and the relative ease of connecting them to diverse protein signaling systems *in vivo* and *in vitro*.[11]

The examples include the construction of protease-activatable autoinhibited signaling modules[12,13] and their integration into ultrasensitive signal amplification circuits.[14] The creation of protease-based artificial receptors and protease-based activated protein reporters[15] enabled the construction of sophisticated and tunable synthetic cellular signaling systems.[16−18] Nevertheless, all reporter designs rely on the construction of a zymogen version of the effector molecule, that is, activating through the process of regulated proteolysis. While this is a broadly applicable approach, the level of engineering effort required for the construction of such

Received: April 24, 2021
Accepted: October 1, 2021
Published: October 12, 2021

https://doi.org/10.1021/acssensors.1c00845
ACS Sens. 2021, 6, 3596–3603

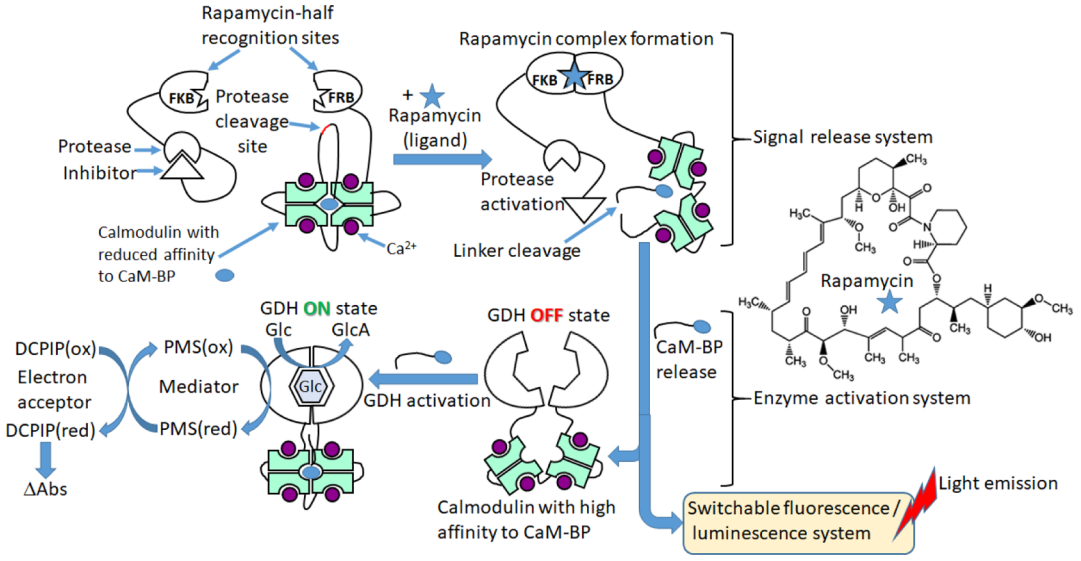

Figure 1. Schematic of the two-component proteolytic signaling system that liberates the caged messenger CaM-BP in a ligand-controlled fashion. Released CaM-BP is able to activate calmodulin-operated artificial allosteric enzymes. The molecular mechanism controlling the activity of CaM-GDH is schematically shown below, left. The light-emitting systems based on CaM-Neon or CaM-NLuc operate similar to the GDH-CaM system and are described in detail elsewhere.[9] The inset shows the molecule structure of rapamycin.

zymogens varies significantly with the choice of the effector molecule.

Another group of proteins that recently became a target of engineering efforts are redox enzymes that can be monitored either through changes in the properties of coreactants or directly by electrochemical methods such as various forms of amperometry.[9] The latter enables their direct connection to the electrochemical systems where they can control other bioelectrochemical processes or bioelectronic devices. Nevertheless, at present, the absolute majority of the engineered systems represent a single switch module that directly converts one signal into another. Here, we present an artificial synthetic signaling cascade that utilizes a ligand-controlled proteolytic system, which generates a messenger molecule capable of selectively activating an artificial allosteric protein reporter. The use of a redox reporter enzyme enabled us to construct a sensory electrode using this system. We discuss further developmental directions for this approach, along with its potential impact.

RESULTS

We recently introduced a generally applicable protein engineering approach for the conversion of constitutively active enzymes into peptide-regulated allosteric switches by inserting a calmodulin (CaM) domain into rationally chosen elements of their secondary structure.[9] This results in inactive chimeric domains that can be activated by calmodulin-binding peptides (CaM-BPs). We also demonstrated that the CaM-BP could be caged inside a low-affinity calmodulin mutant to create a kinetic and thermodynamic barrier and thus control the collision-based reporter activation at high concentrations of the components.[19] Different mechanisms, such as the intermolecular peptide swap and proteolysis, were used to liberate such caged CaM-BPs and activate CaM-operated biosensors.[19,20] These advancements prompted us to test whether the decaging of the CaM-BP could be linked to an arbitrary signal input to build a modular signal transduction cascade. We therefore decided to take advantage of the earlier reported artificial proteolytic system where ligand binding increases the local concentration of the protease substrate in the vicinity of an autoinhibited protease, leading to the cleavage of the former.[13] In order to connect such a system to an output of choice, we endowed it with a protease substrate composed of a "caged" version of the CaM-BP. The proteolytic release of a CaM-BP from the cage enables its interactions with the above-described calmodulin-controlled molecular switches.[9]

To test this idea, we took advantage of a well-characterized chemically induced dimerization system based on rapamycin.[21] We constructed and recombinantly produced a fusion of the FK506-binding (FKB) domain and autoinhibited protease tobacco vein mottling virus (TVMV) protease, as well as a fusion of the FKB protein−rapamycin-binding (FRB) domain with the low-affinity calmodulin mutant connected to the CaM-BP via a flexible linker containing a TVMV protease cleavage site (Figure 1, see also Table S1 in the Supporting Information). The FKB and FRB domains form a ternary complex with rapamycin, thereby bringing the autoinhibited TVMV protease and caged CaM-BP into proximity. High local concentrations of the components are believed to result in the intermolecular swap of the protease inhibitor and protease recognition site, leading to the cleavage of the latter and release of the CaM-BP.[13]

Coupling of Proteolytic Biosensors to Light-Emitting Reporter Systems. The developed two-component protease biosensor architecture is expected to be applicable for all synthetic allosteric reporters operated by calmodulin since the release of the CaM-BP would induce a conformational change in the reporter calmodulin chimera.[9] To experimentally confirm this, we tested the previously developed fluorescent CaM-mNeonGreen (CaM-Neon)[19] and luminescent CaM-NanoLuciferase (CaM-NLuc) as reporter modules.[9] We performed rapamycin titration experiments using solutions of FRB-CaM-CaM-BP and FKB-autoinhibited-TVMV fusion proteins mixed with either CaM-Neon or CaM-NLuc. The affinity of the CaM-BP for its CaM cage is expected to influence the rate of the messenger CaM-BP release, as well as

https://doi.org/10.1021/acssensors.1c00845
ACS Sens. 2021, 6, 3596−3603

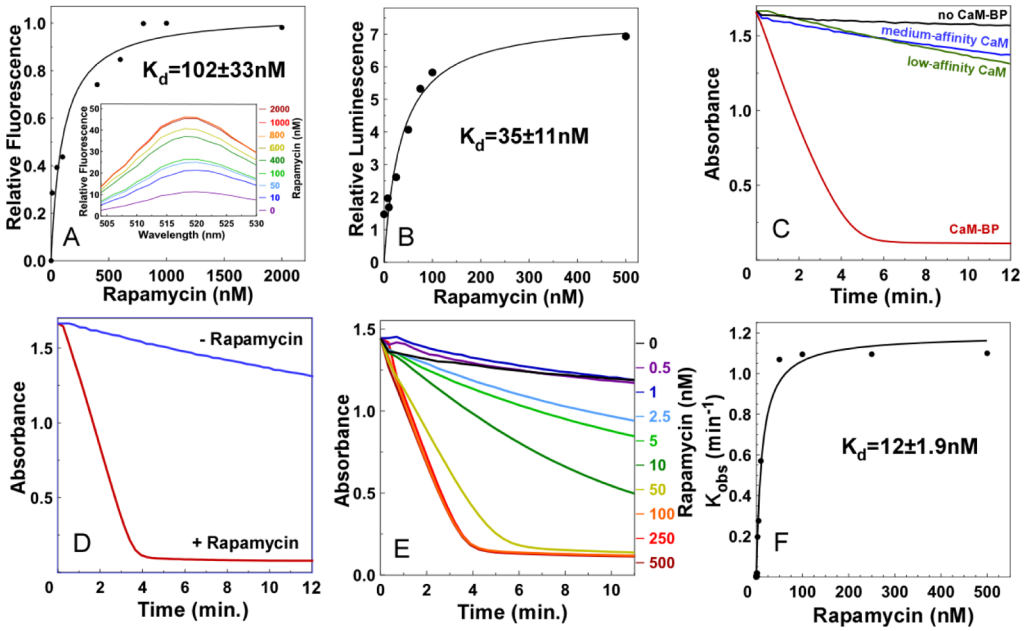

Figure 2. Activation of the calmodulin-operated reporters by the CaM-BP released by a two-component biosensor based on the caged CaM-BP and autoinhibited-TVMV-protease. (A) Titration of 1 μM of CaM-Neon in a mixture of 2 μM FRB-low-affinity-CaM-CaM-BP and 2 μM FKB-autoinhibited-TVMV with increasing concentrations of rapamycin. The relative fluorescence of the resulting mixtures was plotted against rapamycin concentrations and fitted to a quadratic equation, leading to a dose response with a half maximal value of ca. 102 nM and R^2 = 0.94. The inset shows the emission spectra of the same mixture with indicated concentrations of rapamycin. The $\lambda_{ex/em}$ values are 480 and 518 nm. The data points represent the results of a single titration. (B) Titration of a solution of 1 nM CaM-NLuc with a mixture of 50 nM FRB-medium-affinity-CaM-CaM-BP and 50 nM FKB-autoinhibited-TVMV-protease titrated with increasing concentrations of rapamycin. The relative luminescence of the resulting mixtures was plotted against rapamycin concentrations and fitted to a quadratic equation, leading to a dose response with a half maximal value of 35 nM and R^2 = 0.90. The data points represent the values obtained in a single titration experiment. (C) GDH activity of a 10 nM solution of GDH-CaM mixed with 0.5 μM FKB-autoinhibited-TVMV and 0.5 μM FRB-low-affinity-CaM-BP (blue) or 0.5 μM FRB-medium-affinity-CaM-CaM-BP (green). Control reactions were left either unsupplemented (black) or contained 0.2 μM CaM-BP as a positive control (red). The activity of the enzyme was monitored by changes in the absorption of electron-accepting dye DCPIP in the presence of 0.6 mM electron mediator PMS, 20 mM glucose, and 1 mM $CaCl_2$. (D) Biosensor mixture containing a 10 nM solution of GDH-CaM mixed with 0.5 μM FKB-autoinhibited-TVMV and 0.5 μM FRB-low-affinity-CaM-CaM-BP in the absence (blue) or presence (red) of 0.5 μM rapamycin (E) and with different concentrations of rapamycin. (F) Fit of the data from (E) to a quadratic equation leading to a dose response with a half maximal value of 12 nM and R^2 = 0.98. The data points represent the values obtained in a single titration experiment.

the free CaM-BP concentration in the system. Therefore, we tested two (previously described) mutants of CaM referred to as low- and medium-affinity CaM (lCaM and mCaM, respectively) (Table S1 in the Supporting Information).[19] As can be seen in Figure 2A,B, titration of the proteolytic system mixed with luminescent or fluorescent reporters led to a dose-dependent response to rapamycin, indicating that the auto-inhibited protease component could communicate with all CaM-operated chimeras. The apparent affinities of the systems were somewhat different, most likely reflecting the previously observed influence of the reporter domain on the chimera interaction with the CaM-BP.[9]

Testing the Coupling of Proteolytic Biosensors to the GDH-CaM Enzyme Reporter. After demonstrating a successful coupling of the rapamycin-controlled proteolytic biosensor to light-emitting reporter systems, we wanted to test its coupling to the electrochemical pyrroloquinoline quinone (PQQ)-dependent glucose dehydrogenase (GDH)-CaM reporter using a solution colorimetric assay. When the solutions of the recombinant FRB-CaM fusion protein with the CaM-BP caged (lCaM or mCaM)[19] were mixed with equal concentrations of FKB-autoinhibited-TVMV and GDH-CaM chimera, only a slight increase of the GDH activity was observed (Figure 2C). This indicates that the CaM-based cage effectively shielded the CaM-BP from the reporter. As expected, addition of rapamycin led to an increase in GDH activity, indicating the release of the CaM-BP (Figure 2D). The activity levels were similar to that obtained when the reaction solution was spiked with free CaM-BPs (Figure 2C). This indicates that the uncaging process was efficient and that the CaM cage could not sequester significant amounts of cleaved CaM-BPs. The reactions that included the low-affinity cage (lCaM) displayed a faster catalytic rate with the dynamic range calculated to be 16.7-fold, whereas the medium-affinity cage (mCaM) displayed slower activation kinetics with a 12.6-fold dynamic range. The latter is likely due to the slower dissociation of the cleaved CaM-BP from the mCaM cage.

To test the dose dependence of the observed activation on the concentration of the rapamycin ligand, we titrated a fixed amount of the biosensor components with increasing concentrations of rapamycin (Figure 2E). The fit of the observed initial reaction rates to a quadratic equation was used to obtain the apparent dose response value with the half maximum of 12 nM (Figure 2F). This is close to the value previously observed in a rapamycin-controlled two-component GDH biosensor system, confirming that the system operated under single-turnover conditions.[9]

Actuation of Proteolytic Biosensors on GDH-CaM-Functionalized Electrodes. Robust signal conversion by the GDH-CaM reporter prompted us to test if the developed

https://doi.org/10.1021/acssensors.1c00845
ACS Sens. 2021, 6, 3596−3603

signaling system could be integrated with electrochemical devices. To this end, the switchable GDH-CaM chimera was immobilized onto a gold microporous electrode (electrode characterization information provided in Figure S1 in the Supporting Information).[22,23] Initially, the Au-electrode surface was modified with a self-assembled monolayer of 4-mercaptobenzoic acid (4-MBA). Subsequently, the carboxylic groups in the monolayer were used for the covalent attachment of GDH-CaM using a standard carbodiimide procedure (Figure 3).[24] Binding of the CaM-BP to the calmodulin domain of the electrode-immobilized chimeric GDH-CaM system leads to activation of the biocatalytic GDH domain, resulting in an electric current from the glucose oxidation. Note that the covalent binding of GDH-CaM results in a random orientation, with a possible multipoint attachment. It is assumed that only part of the randomly bound enzyme (with a favorable orientation) was capable of direct nonmediated electron transfer to the electrode conductive support.

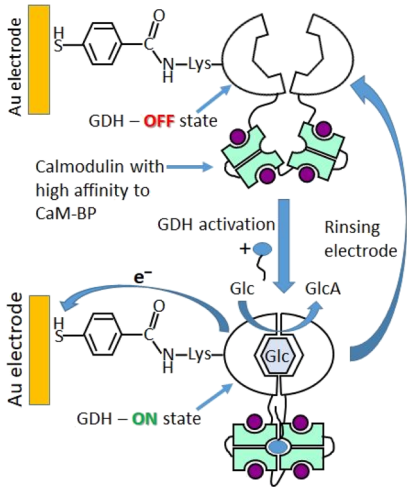

Figure 3. Principle scheme of the GDH-CaM-functionalized electrode operation.

Electrochemical analysis of the electrode-immobilized system reveals that it is catalytically inactive and does not produce current when glucose is present but the CaM-BP is absent (Figure 4A).[25,26] Figure 4A shows a set of cyclic voltammograms (CVs) obtained upon the stepwise addition of the proteolytic biosensor components required for the release of the CaM-BP and subsequent activation of the GDH-CaM-modified electrode. As expected, the system remained electrocatalytically inert (Figure 4A, curves a–e) until all components of the system were added, allowing rapamycin to trigger CaM-BP release from the calmodulin cage. Activation of the electrode-bound GDH-CaM enzyme results in a large increase in the electric current caused by glucose oxidation (Figure 4A, curve f). The electrocatalytic current produced by the system in the active state was obviously dependent on the glucose concentration. However, the system was configured to operate in the presence of a constant saturating glucose concentration of 20 mM. The electric current could be reversibly activated/inhibited by the addition/removal of the activating components to/from the background solution (Figure 4B). The concentration-dependent electrocatalytic current demonstrated linear dependence on the rapamycin concentration in the concentration range of 10–100 nM, with saturation at higher concentrations of the drug (above 500

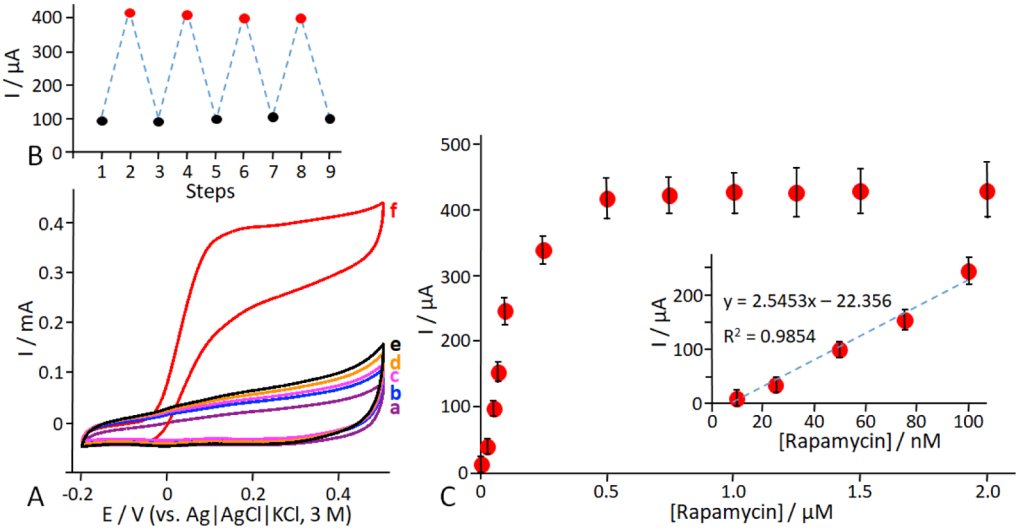

Figure 4. Detection of the rapamycin-induced CaM-BP release using the GDH-CaM bioelectrode: (A) CVs obtained with the GDH-CaM-modified electrode in the presence of different components of the biosensing system: (a) background electrolyte only: HEPES-buffer (25 mM, pH 7.2) with 0.1 M Na_2SO_4; (b) with added 125 μM $Ca(CH_3COO)_2$; (c) with added 20 mM glucose; (d) with added 2.5 μM FKB-autoinhibited-TVMV fusion; (e) with added 2.5 μM FRB-medium affinty-CaM-CaM-BP; and (f) with added 2.5 μM FKB-autoinhibited-TVMV in the presence of 0.5 μM rapamycin. Potential scan rate, 2 mV/s. (B) Reversible activation/inhibition of the bioelectrocatalytic process: Steps 2, 4, 6, and 8 were measured after the addition of all components of the biocatalytic system including rapamycin to the GDH-CaM-modified electrode. Steps 1, 3, 5, 7, and 9 were measured after rinsing the modified electrode with the HEPES-buffer. The currents were measured at E = 0.4 V. (C) Current measured on the GDH-CaM-modified electrode in the solution of 2.5 μM FRB-medium affinity-CaM-CaM-BP, 2.5 μM FKB-autoinhibited-TVMV, and variable concentrations of rapamycin. The inset shows the current obtained at low concentrations of rapamycin. The currents were extracted from the CV (potential scan rate, 2 mV/s) at the potential of 0.4 V. The error bars show the relative standard deviations corresponding to three experiments.

https://doi.org/10.1021/acssensors.1c00845
ACS Sens. 2021, 6, 3596–3603

nM) (Figure 4C). The bioelectrocatalytic system demonstrated good stability (Figure 5A). The activity decrease during

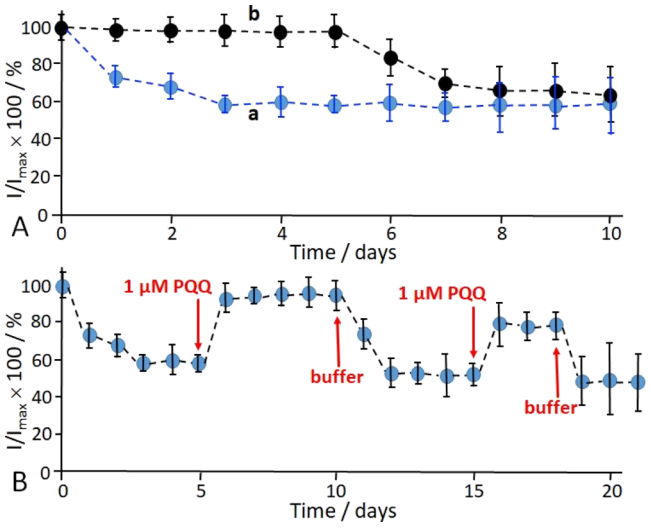

Figure 5. (A) Normalized time-dependent electric current produced by the GDH-CaM electrode stored in the HEPES-buffer, 25 mM, pH 7.2, for 10 days. The current was measured by cyclic voltammetry (at E = 0.4 V) in the absence (a) and presence (b) of 1 μM PQQ in the storage buffer. (B) Effect of the presence or absence of PQQ in the storage buffer solution. Between the measurements, the GDH-CaM-modified electrode was kept in the storage solution at 4 °C.

the first 3 days of storage (Figure 5A, curve a) mostly originated from the leakage of the noncovalently bound PQQ cofactor from the active center of the immobilized GDH-CaM enzyme. This can be mitigated by the addition of 1 μM PQQ to the storage solution (Figure 5A, curve b). The bioelectrocatalytic activity of the GDH-CaM-modified electrode can be reversibly reactivated by the addition of PQQ and then partially inactivated by rinsing the modified electrode with a buffer solution, thus removing part of the PQQ-active center from the immobilized enzyme (Figure 5B).

DISCUSSION

In this study, we tested the idea of utilizing a binding domain/peptide ligand complex as a reusable building block of artificial signaling systems. Using calmodulin/CaM-BP (CaM/CaM-BP), we designed both the signal producing domain in the form of the caged CaM-BP and its receptor in the form of the reporter−calmodulin fusion. We demonstrated that a two-component proteolytic system can be activated by a small-molecule ligand and efficiently release the CaM-BP from the cage. Given the low level of dependence of such systems on the nature of the dimerization system, it is expected that it is possible to engineer similar systems to a broad range of analytes and biochemical activities. Due to their high specificity and the dramatic changes in the physical properties of their substrates, proteases have attracted significant attention of protein and cellular engineers in the recent years,[11] including the use of proteases in various biosensor systems.[12,14,17,18,27]

The present study takes a departure from the designs where the signal-controlled proteolytic reaction activates a zymogen version of the effector polypeptide (for review, see ref 11). Instead, we present a system where a proteolytic biosensor generates a messenger peptide that controls the activity of the effector. This enables the utilization of reporter molecules where the construction of zymogen variants is not straightforward. Furthermore, the use of the messenger peptides potentially endows the system with an additional level of control via its sequestration, degradation, and transport. In the presented example, calmodulin regulates the activity of the reporter domains and enables the released CaM-BP to serve as a messenger molecule connecting the proteolytic signaling system to the reporter. The fact that calmodulin can be used to endow a broad range of reporters with switch-like properties enables the construction of actuators with potentially any output.[9] We experimentally demonstrated the biosensing versatility of the developed system by actuating the proteolytic biosensors on reporter systems with luminescence, fluorescence, optical absorbance (UV−vis), and electrochemical outputs.

One caveat to this system is related to the calcium dependence of the calmodulin module, which serves both as the peptide cage and as the regulatory domain of the reporter. This is less problematic for *in vitro* applications of the developed systems where the concentration of calcium can be tightly controlled. In the case of *in vivo* applications, calcium fluctuation presents a bigger challenge that can be addressed by engineering functional calmodulin variants that are less sensitive to calcium at the physiological intracellular concentration. Another potential pitfall in *in vivo* deployment of calmodulin-operated systems is their potential interaction with the endogenous CaM and CaM-BPs. This, however, may be addressed by deploying engineered CaM/CaM-BP pairs that are orthogonal to the endogenous system.[28]

Furthermore, a similar signaling system can be constructed from other combinations of protein domains and their ligand peptides such as the artificial peptide-binding assembly composed of FN3 and PDZ domains, known as the affinity clamp.[29,30] The use of different regulatory/caging domains enables the construction of signaling systems that are orthogonal to each other.

In principle, this approach should also enable signal amplification, where the proteolytic biosensor releases multiple peptides that then in turn activate catalytic reporter molecules. Under the stoichiometries used and also due to the very high affinity and slow K_{off} of the FRB/rapamycin/FKBP complex, the system tested in this study operated under single-turnover conditions, where the assembly of the FRB/rapamycin/FKB complex resulted in the release of an equimolar amount of the signaling peptide. Utilization of dimerization systems with faster OFF rates, an excess of the caged component, and faster proteases should enable the implementation of signal amplification cascades. Our experimental data strongly suggest that the developed bioelectrodes functionalized with GDH-CaM should enable the quantification of the outputs of such cascades. The sensitivity of GDH-CaM-functionalized bioelectrodes described in this study could be further improved by changing from the random to oriented immobilization of the biosensor on the electrode. A combination of these measures is expected to significantly increase the electrode sensitivity and (in combination with the signal amplification cascades described above) potentially allow the detection of very low concentrations of diverse analytes.

EXPERIMENTAL SECTION

Chemicals and Materials. PQQ, D-(+)-glucose, rapamycin, 4-MBA, gold chloride trihydrate ($AuCl_3 \cdot 3H_2O$), phenazine methosulfate (PMS), 2,6-dichlorophenolindophenol (DCPIP), tris-

https://doi.org/10.1021/acssensors.1c00845
ACS Sens. 2021, 6, 3596−3603

(hydroxymethyl)aminomethane (TRIS-buffer), 4-(2-hydroxyethyl)-1-piperazineethanesulfonic acid (HEPES-buffer), 2-(*N*-morpholino)-ethanesulfonic acid (MES-buffer), and other standard organic and inorganic chemicals and materials were purchased from MilliporeSigma (former Sigma-Aldrich) (St. Louis, MO, USA) or Fisher Scientific (Hampton, NH, USA) and used as supplied without any further purification. The (bio)chemicals used in the preparation of the chimeric enzyme and rapamycin recognition species are detailed elsewhere.[9] Water used in all of the experiments was ultrapure (18.2 MΩ·cm) from a NANOpure Diamond (Barnstead) source. Screen-printed gold electrodes (SPAuE, diameter = 4 mm) were purchased from Metrohm USA (Riverview, FL, USA). The CaM-BP [M13 skeletal muscle myosin light chain kinase peptide (H-Lys-Arg-Arg-Trp-Lys-Lys-Asn-Phe-Ile-Ala-Val-Ser-Ala-Ala-Asn-Arg-Phe-Lys-Lys-Ile-Ser-Ser-Ser-Gly-Ala-Leu-OH; KRRWKKNFIAVSAANRFKKISSS-GAL)] was purchased from AnaSpec, Fremont, CA, USA.

DNA Construction of Chimeric Genes. The chimeric gene of FRB-CaM-CaM-BP was generated by gBlocks from Integrated DNA Technologies, assembled by the Gibson assembly method according to the manufacturer's instructions (New England Biolabs), and cloned into the pET28a vector (see Table S1 in the Supporting Information for the sequences). Construction of the FKB-autoinhibited-TVMV fusion is described elsewhere.[13]

Expression and Purification of Chimeric Proteins. Expression and purification of allosteric reporter proteins (GDH-CaM, CaM-NLuc, and CaM-Neon) and ligand-binding domains FRB and FKB of the fusion chimeric proteins are described elsewhere.[9] All proteins were overexpressed in *E. coli* BL21(DE3)-RIL cells. Cells were grown at 37 °C, and the expression was induced overnight at 18 °C in the presence of 0.3 mM isopropyl thio-β-D-galactoside. Proteins were purified by Ni-NTA chromatography (HIS-Trap FF, ÄKTA Express Purifier, GE Healthcare) at 4 °C. The column was equilibrated with 20 mM TRIS-buffer, 300 mM NaCl, and 20 mM imidazole, pH 8.0. The purified protein was eluted in 20 mM TRIS-buffer, 300 mM NaCl, and 500 mM imidazole, pH 8.0, and dialyzed against a buffer containing 20 mM TRIS-buffer, pH 7.2, and 100 mM NaCl overnight. The purified proteins were concentrated as applicable using Amicon Ultra 10 K MWCO centrifugal filters (EMD Millipore, USA), and aliquoted fractions were stored at −80 °C. The concentrations of the purified proteins were determined using a Nanodrop (Thermo Fisher Scientific) using their calculated molar extinction coefficients at 280 nm based on the amino acid compositions of the final proteins by using the online tool ProtParam (https://www.expasy.org/resources/protparam).

Spectrophotometric Analysis of the GDH-CaM Enzymatic Activity. The GDH-CaM enzyme assay was performed as described previously.[31] Briefly, the assay reaction was performed in polystyrol cuvettes containing 1 mL of the TRIS-buffer (20 mM, pH 7.2) solution of the GDH-CaM enzyme with added 20 mM glucose, 0.6 mM PMS, 0.06 mM DCPIP, 20 mM TRIS-buffer, pH 7.2, 20 mM NaCl, and 1 mM $CaCl_2$. The enzymatic assays were performed at 25 °C by monitoring the decrease in the absorbance of DCPIP at 600 nm using a Cary 50 UV−vis absorbance spectrometer.

Fluorescence Assay. The *in vitro* fluorescence titrations were carried out using a TECAN m1000 PRO plate reader. The assays were performed at 30 °C in a final volume of 200 μL containing 20 mM HEPES-buffer, pH 7.5, 20 mM NaCl, 1 mM $CaCl_2$, and 2 μM caged activator. After 5 min incubation of the reaction mixture, 2 μM FKB-autoinhibited-TVMV-protease, 1 μM CaM-Neon reporter, and indicated concentrations of rapamycin (0−2 μM) were added. After 15 min of incubation time, the CaM-Neon fluorescence was excited at 480 ± 10 nm, and the emission was recorded in 2 nm intervals between 500 and 530 nm. For the dynamic range calculation, the peak intensity of CaM-BP-free CaM-Neon was (518 nm) compared ($\Delta F/F$) with that at the same wavelength after the addition of the ligand.

Luciferase Assay. The reaction mixture was prepared in 200 μL of a TRIS-buffer (20 mM, pH 7.2) solution with the following components: 20 mM NaCl, 0.5 mM $CaCl_2$, and 50 nM FRB-mCaM/CaM-BP. After 5 min incubation, the reaction was supplemented with 1 nM CaM-NLuc enzyme, 50 nM FKB-autoinhibited-TVMV, and the indicated amounts (0−0.5 μM) of rapamycin. Finally, the Nano-Glo luciferase assay reagent was added according to the standard protocol provided by the supplier, and the luminescence was measured using an Infinite F500 reader (Tecan).

Preparation of the GDH-CaM-Modified Electrode. First, a highly porous Au (hPG) electrode was prepared following the procedure detailed recently.[22,23] Briefly, the procedure was as follows: SPAuE (a diameter of 4 mm, Metrohm USA, Riverview, FL, USA) were electrochemically cleaned in 0.1 M H_2SO_4 by performing cyclic voltammetry between −0.3 and +1.7 versus Ag|AgCl|KCl, 3 M, the reference electrode, at a scan rate of 0.3 V s^{-1} until a well-defined CV was obtained. Afterward, the SPAuE were modified by the electrochemical formation of hPG by initially sweeping the potential for 25 scans between +0.8 and 0 V at a scan rate of 50 mV s^{-1} and then applying a fixed potential of −3 V in a 10 mM $AuCl_3$ solution containing 2.5 M NH_4Cl. Then, the modified electrodes were activated in 0.1 M H_2SO_4 by performing cyclic voltammetry between −0.3 and +1.7 V at a scan rate of 0.1 V s^{-1} until a well-defined CV was obtained. The CVs characterizing the electrode before and after the deposition of hPG are shown in Figure S1 in the Supporting Information. The integrated cathodic peak (the charge associated with the peak) observed at ca. +0.9 V is proportional to the effective electrode area.

Then, the modified electrode was incubated overnight in a 10 mM ethanol solution containing 4-MBA. Next, the electrode was thoroughly rinsed with ethanol and distilled water. Afterward, the electrode was incubated with a mixture of 25 mM *N*-hydroxysuccinimide (NHS) and 100 mM 1-ethyl-3-(3-dimethylaminopropyl)-carbodiimide prepared in a phosphate-buffered solution (50 mM, pH 7.2) for 30 min at room temperature (22 ± 2 °C) and subsequently rinsed with a MES-buffer solution (50 mM, pH 6.0) to avoid hydrolysis of the NHS-ester. The functionalized electrodes were immediately incubated with a 1.5 μM GDH-CaM enzyme solution in a HEPES-buffer solution (25 mM, pH 6.0) containing 1 mM $CaCl_2$ for 1 h at room temperature under moderate shaking. The modified electrodes were stored (4 °C) in a HEPES-buffer solution (25 mM, pH 7.2) containing 100 mM Na_2SO_4 until further use.

Electrochemical Experiments. Cyclic voltammetry measurements were carried out with an ECO Chemie Autolab PASTAT 10 electrochemical analyzer using the GPES 4.9 (General Purpose Electrochemical System) software package. A BASi Ag|AgCl|KCl, 3 M, electrode served as the reference electrode, and a graphite slab was used as the counter electrode. CVs were recorded at a scan rate of 2 mV s^{-1} in an electrolyte solution composed of 50 mM HEPES-buffer, pH 7.2, containing 0.1 M Na_2SO_4.

Activation of the Biocatalytic GDH-CaM-Modified Electrode. The electrochemical (cyclic voltammetry) characterization of the GDH-CaM-modified electrode was performed in the following order of the experiments:

a cyclic voltammetry was performed in the background solution composed of the HEPES-buffer (25 mM, pH 7.2) with 0.1 M Na_2SO_4;
b 125 μM $Ca(CH_3COO)_2$ was added to the background solution, and the CV was remeasured;
c 20 mM glucose was added, and the CV was remeasured;
d the 2.5 μM FKB domain linked to the autoinhibited protease was added, and the CV was remeasured;
e the 2.5 μM FRB domain linked to the medium affinity-CaM-CaM-BP was added, and the CV was remeasured; and
f after that, the reactant mixture was incubated for 20 min prior to the addition of rapamycin; then, rapamycin was added with different concentrations (in the range 10−2000 nM starting from the smallest and then increased); and the CVs were measured for all concentrations of the added rapamycin (the results are shown in Figure 4).

Stability Measurements for the Activated PQQ-GDH-CaM-Modified Electrode. After the enzyme-modified electrode was activated with a saturated concentration of rapamycin (1 μM), the stability measurements were performed over 10 or 20 days (Figure 5).

https://doi.org/10.1021/acssensors.1c00845
ACS Sens. 2021, 6, 3596−3603

Between the measurements, the modified electrode was stored in a buffer solution at 4 °C. Two different storage buffer solutions were used: (i) 25 mM HEPES-buffer, pH 7.2, and (ii) 25 mM HEPES-buffer, pH 7.2, containing 1 μM PQQ. In another experiment, the modified electrode was stored with the HEPES-buffer without added PQQ, and the electrode was treated with the 1 μM PQQ solution or rinsed with the HEPES-buffer prior to the cyclic voltammetry measurements.

■ ASSOCIATED CONTENT

Supporting Information

The Supporting Information is available free of charge at https://pubs.acs.org/doi/10.1021/acssensors.1c00845.

Experimental data and sequences of the artificial proteins used in the study (PDF)

■ AUTHOR INFORMATION

Corresponding Authors

Kirill Alexandrov − *CSIRO-QUT Synthetic Biology Alliance, ARC Centre of Excellence in Synthetic Biology, Centre for Agriculture and the Bioeconomy, Centre for Genomics and Personalised Health, School of Biology and Environmental Science, Queensland University of Technology, Brisbane, Queensland 4001, Australia*; Email: kirill.alexandrov@qut.edu.au

Evgeny Katz − *Department of Chemistry and Biomolecular Science, Clarkson University, Potsdam, New York 13699, United States*; orcid.org/0000-0002-1618-4620; Email: ekatz@clarkson.edu

Authors

Paolo Bollella − *Department of Chemistry and Biomolecular Science, Clarkson University, Potsdam, New York 13699, United States; Department of Chemistry, University of Bari A. Moro, Bari 70125, Italy*; orcid.org/0000-0001-9049-6406

Selvakumar Edwardraja − *Australian Institute for Bioengineering and Nanotechnology, University of Queensland, Brisbane, Queensland 4072, Australia*

Zhong Guo − *CSIRO-QUT Synthetic Biology Alliance, ARC Centre of Excellence in Synthetic Biology, Centre for Agriculture and the Bioeconomy, Centre for Genomics and Personalised Health, School of Biology and Environmental Science, Queensland University of Technology, Brisbane, Queensland 4001, Australia*

Claudia E. Vickers − *CSIRO Synthetic Biology Future Science Platform, Brisbane, Queensland 4001, Australia*; orcid.org/0000-0002-0792-050X

Jason Whitfield − *Australian Institute for Bioengineering and Nanotechnology, University of Queensland, Brisbane, Queensland 4072, Australia*

Patricia Walden − *CSIRO-QUT Synthetic Biology Alliance, ARC Centre of Excellence in Synthetic Biology, Centre for Agriculture and the Bioeconomy, Centre for Genomics and Personalised Health, School of Biology and Environmental Science, Queensland University of Technology, Brisbane, Queensland 4001, Australia*

Artem Melman − *Department of Chemistry and Biomolecular Science, Clarkson University, Potsdam, New York 13699, United States*; orcid.org/0000-0003-1152-972X

Complete contact information is available at: https://pubs.acs.org/10.1021/acssensors.1c00845

Author Contributions

P.B. and S.E. contributed equally. P.B. performed electrochemical measurements; S.E., Z.G., and J.W. prepared and characterized the biomolecule components and performed the optical absorbance and fluorescence measurements; A.M. and K.A. were responsible for the experimental design and general supervision of the project; and E.K. supervised the electrochemical part of the project.

Notes

The authors declare the following competing financial interest(s): KA holds equity and serves as a director and Chief Scientific officer of Molecular Warehouse Inc. that holds patents covering PQQ-GDH-CaM chimeras. ZG is a co-inventor on those patents.

■ ACKNOWLEDGMENTS

This work was supported in part by the Australian Research Council Discovery Projects DP160100973 and DP150100936 as well as the ARC Centre of Excellence in Synthetic Biology CE200100029 to K.A. This work was also supported by the NHMRC Development grants APP1113262 to K.A. and APP1179001 to K.A. This work was also in part supported by the HFSP grant RGP0002/2018 to K.A. and E.K. and the US Department of Defense grant W81XWH-20-1-0708 to K.A., E.K., and A.M. K.A. gratefully acknowledges the financial support of the CSIRO-QUT Synthetic Biology Alliance. Authors are grateful to Dr. Wayne A. Johnston for critically reading the manuscript.

■ ABBREVIATIONS

4-MBA, 4-mercaptobenzoic acid; CaM, calmodulin (calcium-modulated protein); CaM-BP, (M13 skeletal muscle myosin light chain kinase peptide); CaM-Neon, calmodulin fused with the mNeonGreen dye; CaM-NLuc, calmodulin fused with nanoluciferase; CV, cyclic voltammogram; DCPIP, 2,6-dichlorophenolindophenol; EDC, 1-ethyl-3-(3-dimethylaminopropyl)carbodiimide (carbodiimide coupling reagent); FKB, FK506-binding protein; FRB, FKBP−rapamycin binding protein; FN3, Fibronectin type III domain; GDH, PQQ-dependent glucose dehydrogenase (E.C. 1.1.5.2); GDH-CaM, GDH fused with the CaM chimeric enzyme; HEPES, 4-(2-hydroxyethyl)-1-piperazineethanesulfonic acid (buffer); hPG, highly porous gold; lCaM, calmodulin derivative with low affinity for CaM-BP; mCaM, calmodulin derivative with medium affinity for CaM-BP; MES, 2-(*N*-morpholino)-ethanesulfonic acid (buffer); NHS, *N*-hydroxysuccinimide; NLuc, nanoluciferase (luminescent enzyme); PDZ, PDZ domain; PMS, phenazine methosulfate; PQQ, pyrroloquinoline quinone (active center of GDH); SPAuE, screen-printed gold electrodes; TRIS, tris(hydroxymethyl)aminomethane (buffer); TVMV, protease tobacco vein mottling virus protease

■ REFERENCES

(1) Dixon, T. A.; Williams, T. C.; Pretorius, I. S. Sensing the future of bio-informational engineering. *Nat. Commun.* **2021**, *12*, 388.

(2) Kucherenko, I. S.; Soldatkin, O. O.; Dzyadevych, S. V.; Soldatkin, A. P. Electrochemical biosensors based on multienzyme systems: Main groups, advantages and limitations − A review. *Anal. Chim. Acta* **2020**, *1111*, 114−131.

(3) Wang, Z.; Sekar, B. S.; Li, Z. Recent advances in artificial enzyme cascades for the production of value-added chemicals. *Bioresour. Technol.* **2021**, *323*, 124551.

(4) *Implantable Bioelectronics − Devices, Materials, and Applications*; Katz, E., Ed.; Wiley-VCH: Weinheim, 2014.
(5) *Wearable Bioelectronics*; Parlak, O.; Salleo, A.; Turner, A., Eds.; Elsevier: Amsterdam, 2020.
(6) Yeh, H.-W.; Ai, H.-W. Development and applications of bioluminescent and chemiluminescent reporters and biosensors. *Annu. Rev. Anal. Chem.* **2019**, *12*, 129−150.
(7) Zhou, X.; Mehta, S.; Zhang, J. Genetically encodable fluorescent and bioluminescent biosensors light up signaling networks. *Trends Biochem. Sci.* **2020**, *45*, 889−905.
(8) Kostyuk, A. I.; Demidovich, A. D.; Kotova, D. A.; Belousov, V. V.; Bilan, D. S. Circularly permuted fluorescent protein-based indicators: History, principles, and classification. *Int. J. Mol. Sci.* **2019**, *20*, 4200.
(9) Guo, Z.; Johnston, W. A.; Whitfield, J.; Walden, P.; Cui, Z.; Wijker, E.; Edwardraja, S.; Lantadilla, I. R.; Ely, F.; Vickers, C.; Ungerer, J. P. J.; Alexandrov, K. Generalizable protein biosensors based on synthetic switch modules. *J. Am. Chem. Soc.* **2019**, *141*, 8128−8135.
(10) Stein, V.; Alexandrov, K. Synthetic protein switches: design principles and applications. *Trends Biotechnol.* **2015**, *33*, 101−110.
(11) Gräwe, A.; Ranglack, J.; Weber, W.; Stein, V. Engineering artificial signalling functions with proteases. *Curr. Opin. Biotechnol.* **2020**, *63*, 1−7. (and references therein)
(12) Aper, S. J. A.; den Hamer, A.; Wouters, S. F. A.; Lemmens, L. J. M.; Ottmann, C.; Brunsveld, L.; Merkx, M. Protease-activated scaffold protein as versatile molecular hubs in synthetic signalling networks. *ACS Synth. Biol.* **2018**, *7*, 2216−2225.
(13) Stein, V.; Alexandrov, K. Protease-based synthetic sensing and signal amplification. *Proc. Natl. Acad. Sci. U.S.A.* **2014**, *111*, 15934−15939.
(14) Stein, V.; Nabi, M.; Alexandrov, K. Ultrasensitive scaffolds-dependent protease sensors with large dynamic range. *ACS Synth. Biol.* **2017**, *6*, 1337−1342.
(15) Zhang, Q.; Schepis, A.; Huang, H.; Yang, J.; Ma, W.; Torra, J.; Zhang, S.-Q.; Yang, L.; Wu, H.; Nonell, S.; Dong, Z.; Kornberg, T. B.; Coughlin, S. R.; Shu, X. Designing a green fluorogenic protease reporter by flipping a beta strand of GFP for imaging apoptosis in animals. *J. Am. Chem. Soc.* **2019**, *141*, 4526−4530.
(16) Schwarz, K. A.; Daringer, N. M.; Dolberg, T. B.; Leonard, J. N. Rewiring human cellular input−output using modular extracellular sensors. *Nat. Chem. Biol.* **2017**, *13*, 202−209.
(17) Gao, X. J.; Chong, L. S.; Kim, M. S.; Elowitz, M. B. Programmable protein circuits in living cells. *Science* **2018**, *361*, 1252−1258.
(18) Fink, T.; Lonzarić, J.; Praznik, A.; Plaper, T.; Merljak, E.; Leben, K.; Jerala, N.; Lebar, T.; Strmšek, Ž.; Lapenta, F.; Benčina, M.; Jerala, R. Design of fast proteolysis-based signaling and logic circuits in mammalian cells. *Nat. Chem. Biol.* **2019**, *15*, 115−122.
(19) Edwardraja, S.; Guo, Z.; Whitfield, J.; Lantadilla, I. R.; Johnston, W. A.; Walden, P.; Vickers, C. E.; Alexandrov, K. Caged activators of artificial allosteric protein biosensors. *ACS Synth. Biol.* **2020**, *9*, 1306−1314.
(20) Bollella, P.; Edwardraja, S.; Guo, Z.; Alexandrov, K.; Katz, E. Control of allosteric electrochemical protein switch using magnetic signals. *Chem. Commun.* **2020**, *56*, 9206−9209.
(21) Banaszynski, L. A.; Liu, C. W.; Wandless, T. J. Characterization of the FKBP.rapamycin.FRB ternary complex. *J. Am. Chem. Soc.* **2005**, *127*, 4715−4721.
(22) Bollella, P. Porous Gold: A new frontier for enzyme-based electrodes. *Nanomaterials* **2020**, *10*, 722.
(23) Bollella, P.; Hibino, Y.; Kano, K.; Gorton, L.; Antiochia, R. Highly sensitive membraneless fructose biosensor based on fructose dehydrogenase immobilized onto aryl thiol modified highly porous gold electrode: Characterization and application in food samples. *Anal. Chem.* **2018**, *90*, 12131−12136.
(24) Willner, I.; Katz, E. Integration of layered redox-proteins and conductive supports for bioelectronic applications. *Angew. Chem., Int. Ed. Engl.* **2000**, *39*, 1180−1218.
(25) Bollella, P.; Edwardraja, S.; Guo, Z.; Kirill Alexandrov, K.; Katz, E. Control of allosteric protein electrochemical switches with biomolecular and electronic signals. *J. Phys. Chem. Lett.* **2020**, *11*, 5549−5554.
(26) Gamella, M.; Guo, Z.; Alexandrov, K.; Katz, E. Bioelectrocatalytic electrodes modified with PQQ-glucose dehydrogenase−calmodulin chimera switchable by peptide signals: Pathway to generic bioelectronic systems controlled by biomolecular inputs. *ChemElectroChem* **2019**, *6*, 638−645.
(27) Shekhawat, S. S.; Porter, J. R.; Sriprasad, A.; Ghosh, I. An autoinhibited coiled-coil design strategy for split-protein protease sensors. *J. Am. Chem. Soc.* **2009**, *131*, 15284−15290.
(28) Shifman, J. M.; Mayo, S. L. Exploring the origins of binding specificity through the computational redesign of calmodulin. *Proc. Natl. Acad. Sci. U.S.A.* **2003**, *100*, 13274−13279.
(29) Huang, J.; Koide, A.; Makabe, K.; Koide, S. Design of protein function leaps by directed domain interface evolution. *Proc. Natl. Acad. Sci. U.S.A.* **2008**, *105*, 6578−6583.
(30) Bollella, P.; Bellare, M.; Kadambar, V. K.; Guo, Z.; Alexandrov, K.; Melman, A.; Katz, E. Boolean logic networks mimicked with chimeric enzymes activated/inhibited by several input signals. *ChemPhysChem* **2020**, *21*, 589−593.
(31) Guo, Z.; Murphy, L.; Stein, V.; Johnston, W. A.; Alcala-Perez, S.; Alexandrov, K. Engineered PQQ-glucose dehydrogenase as a universal biosensor platform. *J. Am. Chem. Soc.* **2016**, *138*, 10108−10111.

https://doi.org/10.1021/acssensors.1c00845
ACS Sens. 2021, 6, 3596−3603